Determination of Activation and Deactivation Rate Constants of Model Compounds in Atom Transfer Radical Polymerization[1]

Krzysztof Matyjaszewski,* Hyun-jong Paik,† Peng Zhou, and Steve J. Diamanti

Center for Macromolecular Engineering, Department of Chemistry, Carnegie Mellon University, 4400 Fifth Avenue, Pittsburgh, Pennsylvania 15213

Received January 31, 2001

ABSTRACT: The activation and deactivation rate constants in atom transfer radical polymerization (ATRP) were measured using model compounds. The activation rate constants were determined using HPLC or GC under the kinetic isolation condition achieved by trapping the generated radical with 2,2,6,6-tetramethylpiperidinyl-1-oxy (TEMPO). The deactivation rate constants were measured by trapping 1-phenylethyl radicals with TEMPO in a competitive reaction. The effects of several parameters in ATRP systems were examined, including alkyl groups, ligands, transferred groups, and solvents. The data obtained were consistent with ATRP kinetics and provided further quantitative insights into understanding the ATRP processes.

Introduction

One method used to generate a free radical is a metal-catalyzed atom transfer reaction, where homolytic cleavage of the bond between the carbon and the heteroatom occurs through transfer of the heteroatom to the metal complex accompanied by oxidation of the metal center.[2] This route has been used extensively in organic synthesis and has been named atom transfer radical addition (ATRA). In ATRA,[3] a generated radical adds to an unsaturated substrate, followed by atom transfer back to the adduct. Recent extension of this concept to radical polymerization, i.e., atom transfer radical polymerization (ATRP), has opened new possibilities for the preparation of novel polymeric architectures in a controlled fashion via a radical process.[4−6]

The basic concept behind ATRP is the reversible formation of a radical by transfer of a halogen from an alkyl halide to a transition metal complex (Scheme 1).[7,8] Through this reversible formation of active radicals from dormant alkyl halides, ATRP controls polymer properties, such as molecular weight, molecular weight distribution, chain end functionality, composition, and topology.

The success of ATRP depends largely on an appropriate equilibrium between the activation process (generation of radicals, k_{act}) and the deactivation process (formation of alkyl halides, k_{deact}). The equilibrium between the two processes ($K_{eq} = k_{act}/k_{deact}$) determines the concentration of radicals and subsequently the rates of polymerization and termination. Usually K_{eq} is very small, which maintains a low radical concentration and minimizes termination reactions. At the same time, each rate constant (k_{act} and k_{deact}) affects the level of control in the polymerization. Ideally, both k_{act} and k_{deact} should be large enough (though $k_{act} \ll k_{deact}$) to provide good control over the polymerization while maintaining a reasonable polymerization rate.

ATRP is a complex system due to the many variables in the polymerization system. For the successful ATRP of a particular monomer, it is necessary to carefully adjust many internal variables including structures and concentrations of initiators (RX), metals (Mt^n), ligands (L), transferred atoms or groups (X), and solvents, as well as external variables such as temperature and reaction time[8,9] (Scheme 1). The overall rate of polymerization and the level of control during the polymerization are influenced by the choice of these variables through affecting k_{act} and k_{deact}. Therefore, it is important to know the values of k_{act} and k_{deact} under various conditions for successful ATRP and further development of new ATRP systems.

Scheme 1. Elementary Reactions of ATRP

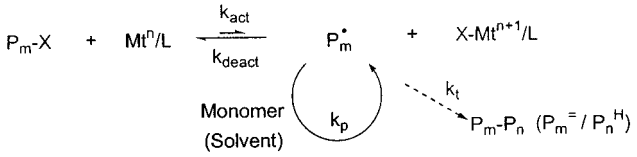

Despite the importance of these rate constants, very few measurements have been made so far. For polymeric and monomeric systems, k_{act} was measured using spectroscopic[10] or chromatographic techniques.[11−13] The deactivation rate constants have been even less extensively studied. Although the deactivation rate constant was estimated for bromo-terminated polystyrene based on the polymerization rate[11] and evolution of polydispersities with conversion,[14,15] it has not been directly measured for the ATRP system. There are a few data on trapping primary alkyl radicals by cupric halides.[16] This is partially due to the lack of reliable and expedient methods to determine the rate constants of very fast reactions such as atom transfer.

Here, we report methods developed to measure k_{act} and k_{deact}. This paper reports the rate constants for model compounds of several different types of polymeric chain ends under various conditions (i.e., different ligands, solvents, and transferred groups) using trapping methods.

Description of Methods

Activation Rate Constant Measurements. The rate constant k_{act} was determined by kinetically isolating the activation process (1) from the deactivation

† Current address: Nanobiotechnology Center, Cornell University, Ithaca, NY 14853.

10.1021/ma010185+ CCC: $20.00
Published on Web 06/19/2001

Scheme 2. Model Reaction for Measurements of the Activation Rate Constant

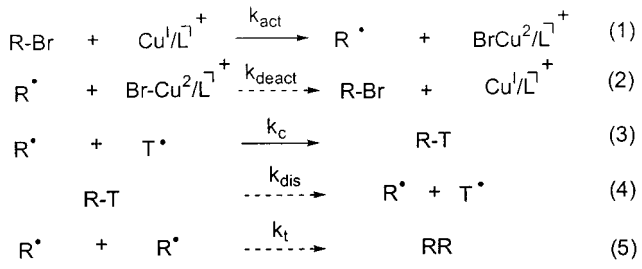

process (2) (Scheme 2). After radical R* was generated through an atom transfer process (1), it was exclusively trapped with an excess amount of 2,2,6,6-tetramethylpiperidinyl-1-oxy (TEMPO, T*) (3), yielding an alkoxyamine (R−T). The contributions of the deactivation step (2), thermal dissociation of R−T (4), and self-coupling (5) were negligible due to the low Cu(II)Br_2/L concentration, the smaller rate constant (k_{dis}),[17,18] and the lower radical concentration, respectively. Under these conditions, the rate of activation should be the same as the rate of consumption of R−Br and the rate of formation of R−T. The change in the concentration of R−Br and R−T with time was monitored using HPLC (Figure 1). The concentrations of alkyl bromide (1-phenylethyl bromide, PEBr) decreased and alkoxyamine (1-(2,2,6,6-tetramethylpiperidinyloxy)-1-phenylethane, PETEMPO) increased with time. Biphenyl was used as an internal standard. Similar approaches have been reported for determining the dissociation rate constants of alkoxyamines[17,19,20] and the activation reaction rate constants for (polymeric) alkyl halides.[10,12,13]

An excess amount of catalyst (20 times with respect to R−Br) was used to provide pseudo-first-order kinetic conditions. The first-order kinetic plot of the consumption of R−Br was almost linear (Figure 2a), indicating that the change in concentration of the catalyst was relatively small during the reaction while reactions 2 and 4 did not contribute significantly. The slope of the pseudo-first-order kinetic plot is equal to the apparent rate constant, which is the product of the catalyst concentration and the activation rate constant (eq 1).

$$-\frac{d[RBr]}{dt} \approx k_{act}[Cu(I)Br][RBr] = k_{app}[RBr] \quad (\text{where } k_{act}[Cu(I)Br] = k_{app}) \quad (1)$$

Comparing the conversion of R−Br and the yield of R−T confirmed that R−Br was almost quantitatively converted to R−T, which remained intact throughout the reaction (Figure 2b). Potential side reactions include the loss of hydrogen bromide[21] and the formation of hydroxylamine with generation of an unsaturated product from R−T.[22,23] However, we ignored these side reactions in the present analysis, since their relative rates were much slower than that of the activation process under the given conditions.

HPLC analysis is a reliable method for measuring activation rate constants for certain UV active model compounds such as 1-phenylethyl bromide (PEBr) and benzyl bromide (BzBr). However, compounds such as ethyl 2-bromoisobutyrate (EBriB) and methyl 2-bromopropionate (MBrP) were difficult to analyze by HPLC due to their low extinction coefficients.

The use of GC was an attractive alternative since it detects all the model compounds without the need for a UV chromophore. Furthermore, several alkyl halides could be studied simultaneously, due to sufficient separation of the substrates by GC. Figure 3 shows (a) GC results and (b) first-order kinetic plots of four model compounds obtained simultaneously from GC results. This approach allowed successful and expedient assaying of several model compounds representing dormant species in the ATRP of various monomers. The data given below were obtained using either HPLC or GC, depending on the structure of the model compound.

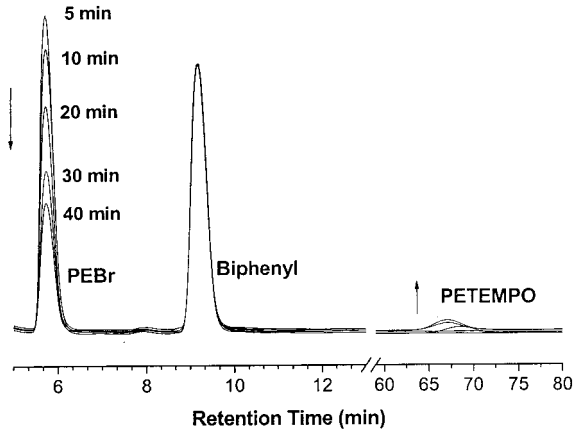

Figure 1. HPLC traces in activation rate constant measurements. $[PEBr]_0 = 1.0 \times 10^{-3}$ M, $[Cu(I)Br]_0 = [dNbpy]_0/2 = 2.0 \times 10^{-2}$ M, $[TEMPO]_0 = 4.0 \times 10^{-2}$ M, $[biphenyl]_0 = 1.0 \times 10^{-3}$ M in ethyl acetate at 42 °C; see Experimental Section for HPLC conditions.

Deactivation Rate Constant Measurements. Values of k_{deact} were measured using a competitive kinetic experiment in which the radical generated was coupled with TEMPO as a clock reaction (Scheme 3). 1-Phenylethyl radical (PE) reacted with TEMPO and the Cu(II)Br_2 complex to yield PETEMPO and PEBr, respectively. By comparing the amount of these two products formed (PEBr and PETEMPO), the deactivation rate constants (k_{deact}) were calculated relative to the combination rate constant (k_{comb2}) available in the literature[24−26] (eq 2).

$$\frac{d[PEBr]}{d[PETEMPO]} = \frac{k_{deact}}{k_{comb2}} \frac{[Cu(II)Br_2/L][PE^*]}{[TEMPO][PE^*]} \quad (2)$$

$$k_{deact} = k_{comb2} \frac{[TEMPO]}{[Cu(II)Br_2/L]} \frac{[PEBr]}{d[PETEMPO]}$$

The PE radical was produced by thermal dissociation of 1-(*N*,*N*−(2-methylpropyl-1)-(1-diethylphosphono-2,2-dimethylpropyl-1-)-*N*-oxyl)-1-phenylethane (PESG1).[18,27−29] The recently developed nitroxide (SG1) provides two advantages to this experiment. First, the large dissociation rate constant ($k_{dis1} = 4.0 \times 10^{-5}$ M^{-1} s^{-1}) at a relatively low temperature, 75 °C, ensured sufficient generation of radicals without significant decomposition of PETEMPO ($k_{dis2} = 2.8 \times 10^{-6}$ M^{-1} s^{-1}).[26] Second, the smaller combination rate constant ($k_{comb1} = 5.6 \times 10^{6}$ M^{-1} s^{-1}) minimized its interference with the trapping reactions.[26]

The consumption of PESG1 and the formation of PEBr and PETEMPO were monitored simultaneously using HPLC (Figure 4). The diastereomers of the PESG1 (Scheme 3) were separated in the HPLC analysis, and the rates of the dissociation of each diastereomers (k_{dis1}) were similar.

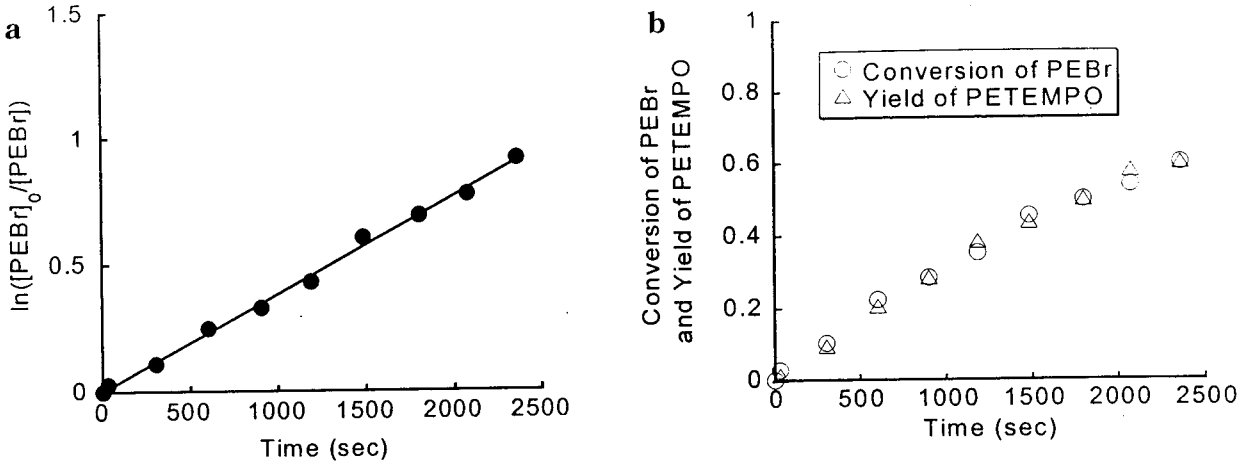

Figure 2. (a) First-order kinetic plot in activation rate constant measurement. (b) Consumption of PEBr and formation of PETEMPO. $[PEBr]_0 = 1.0 \times 10^{-3}$ M, $[Cu(I)Br]_0 = [dNbpy]_0/2 = 2.0 \times 10^{-2}$ M, $[TEMPO]_0 = 4.0 \times 10^{-2}$ M, $[biphenyl]_0 = 1.0 \times 10^{-3}$ M in ethyl acetate at 42 °C. Conversion of PEBr (○). Yield of PETEMPO (△).

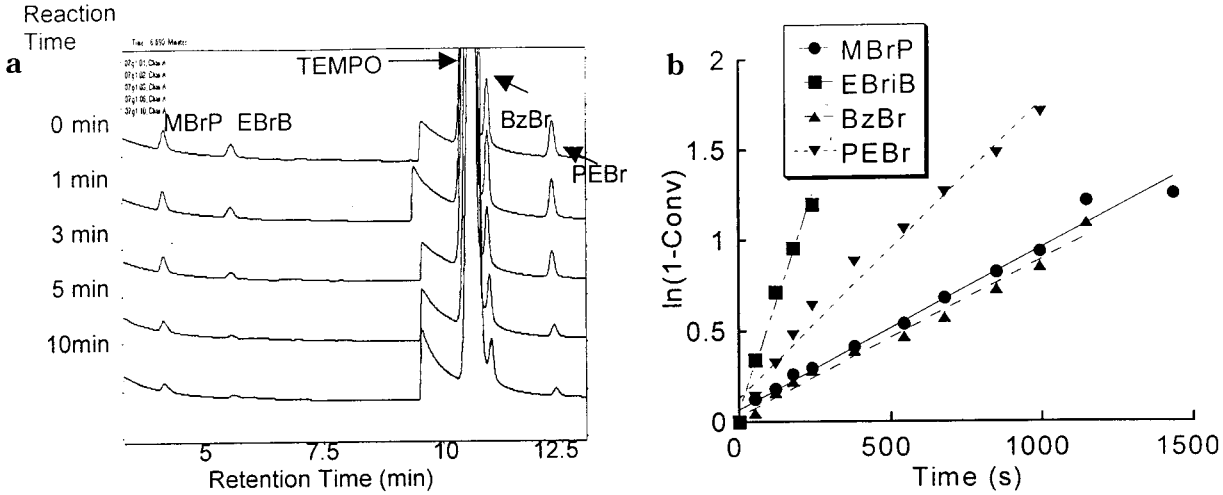

Figure 3. (a) GC traces and (b) kinetic plot of the activation experiment with Cu(I)Br/dNbpy, $[PEBr]_0 = [BzBr]_0 = [MBrP]_0 = [EBriB]_0 = 5.0 \times 10^{-4}$ M, $[Cu(I)Br]_0 = [dNbpy]_0/2 = 2.0 \times 10^{-2}$ M, $[TEMPO]_0 = 2.0 \times 10^{-2}$ M, $[biphenyl]_0 = 5.0 \times 10^{-4}$ M in ethyl acetate at 70 °C.

Scheme 3. Model Reaction for Measurements of the Deactivation Rate Constant

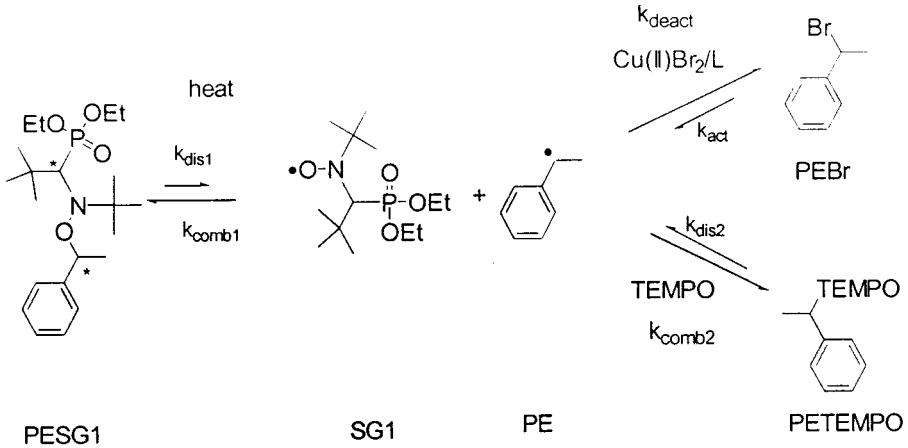

Figure 5 shows the relative mole ratios of PEBr and PETEMPO against time. The mole ratio of the two products decreased with time. The PEBr formed was consumed through the activation process with the reduced catalyst after the atom transfer reaction. Additionally, the decrease in the mole ratio of the two products may also be attributed to the formation of styrene from PEBr in the presence of $Cu(II)Br_2$/dNbpy, as seen in Figure 4 and as observed previously.[21] However, we did not take these reactions into an account in our analysis, because their overall contribution was insignificant in the early stage of the reactions. We used the average mole ratio of PEBr/PETEMPO within 2 h for our calculation of k_{deact}.

When the initial mole ratio of $Cu(II)Br_2$ and TEMPO increased, the mole ratio of two products, PEBr and

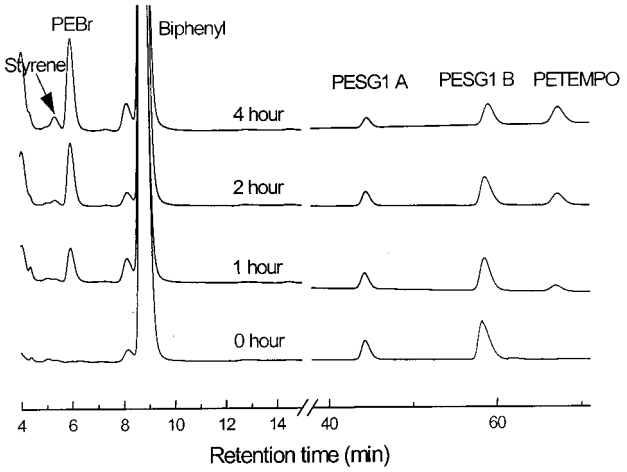

Figure 4. Typical HPLC traces for deactivation experiments: $[PESG1]_0 = 1.0 \times 10^{-3}$ M, $[Cu(II)Br_2]_0 = {}^1/_2[dNbpy]_0 = 1.0 \times 10^{-2}$ M, $[TEMPO]_0 = 3.0 \times 10^{-3}$ M, $[biphenyl]_0 = 1.0 \times 10^{-3}$ M (internal standard) in acetonitrile at 75 °C; see Experimental Section for HPLC conditions.

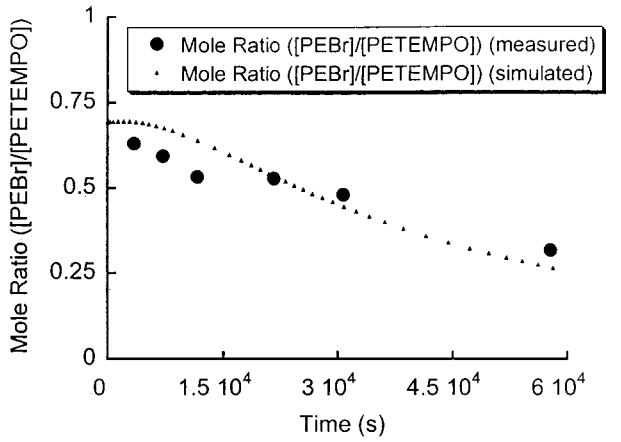

Figure 5. Change of the mole ratio of [PEBr]/[PETEMPO] with time: measured (●) and simulated (▲); $[PESG1]_0 = 1.0 \times 10^{-3}$ M, $[Cu(II)Br_2]_0 = {}^1/_2[dNbpy]_0 = 1.0 \times 10^{-2}$ M, $[TEMPO]_0 = 3.0 \times 10^{-3}$ M, $[biphenyl]_0 = 1.0 \times 10^{-3}$ M (internal standard) in acetonitrile at 75 °C.

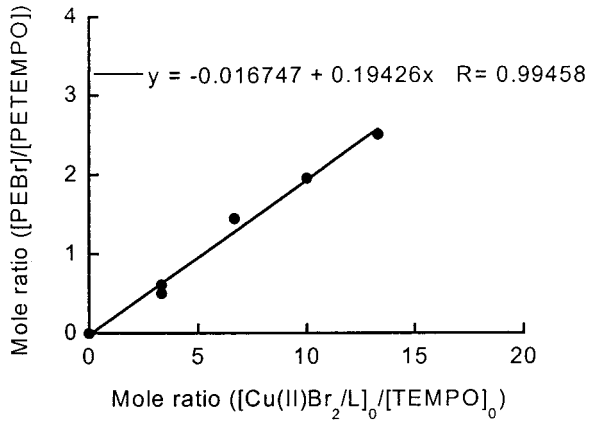

Figure 6. Plot of the mole ratio ([PEBr]/[PETEMPO]) vs initial concentration ratio of $[Cu(II)Br_2/L]_0/[TEMPO]_0$ in acetonitrile at 75 °C.

PETEMPO, increased linearly (Figure 6). Again the mole ratios of the two products were determined by averaging the mole ratios obtained over 2 h. This linear relationship shows that eq 2 holds over a wide range of the initial concentration ratios between $Cu(II)Br_2/L$ and

Table 1. Activation Rate Constants Measured under Various Conditions at 35 °C

no.	RX	complex	solvent	k_{act} [M^{-1} s^{-1}]
1	PEBr	CuBr/2dNbpy	acetonitrile	0.085
2	MBrP	CuBr/2dNbpy	acetonitrile	0.052
3	EBriB	CuBr/2dNbpy	acetonitrile	0.60
4	BzBr	CuBr/2dNbpy	acetonitrile	0.043
5	PEBr	CuBr/PMDETA	acetonitrile	0.12
6	MBrP	CuBr/PMDETA	acetonitrile	0.11
7	EBriB	CuBr/PMDETA	acetonitrile	1.7
8	PECl	$CuCl/Me_6TREN$	acetonitrile	1.5
9	PEBr	CuBr/2dNbpy	ethyl acetate	0.016
10	PECl	CuCl/2dNbpy	acetonitrile	0.000056

Table 2. Deactivation Rate Constants under Various Conditions at 75 °C

no.	radical	complex	solvent	k_{deact} [M^{-1} s^{-1}]
1	PE	$Cu(II)Br_2/2dNbpy$	acetonitrile	2.5×10^7 [a]
2	PE	$Cu(II)Br_2/PMDETA$	acetonitrile	6.1×10^6 [a]
3[c]	PE	$Cu(II)Br_2/Me_6TREN$	acetonitrile	1.4×10^7 [a]
4	PE	$Cu(II)Br_2/2dNbpy$	ethyl acetate	2.4×10^8 [b]
5	PE	$Cu(II)Cl_2/2dNbpy$	acetonitrile	4.3×10^6 [a]

[a] Calculated based on $k_{comb2} = 1.3 \times 10^8$ M^{-1} s^{-1};[24] the temperature dependence of the k_{comb2} was not taken into account owing to the low activation energy of the combination reaction. [b] Calculated based on $k_{comb2} = 2.4 \times 10^8$ M^{-1} s^{-1};[24–26] since k_{comb2} values in ethyl acetate (EA) were not available, the scaling of k_{comb2} in acetonitrile (ACN) for $k_{comb2,EA}$ was made with correcting factor 1.8 ($k_{comb2,EA}/k_{comb2,ACN}$). The correcting factor was based on the ratio $k_{comb2,EA}/k_{comb2,ACN}$ reported for the reaction between benzyl radial and TEMPO. [c] Measured with exposure to air.

TEMPO. The deactivation rate constant $k_{deact} = 2.5 \times 10^7$ M^{-1} s^{-1} was determined from the slope in Figure 6 based on $k_{comb2} = 1.3 \times 10^8$ M^{-1} s^{-1}.[24]

In the deactivation rate constant measurement with Me_6TREN complex, the consumption of PEBr formed by reduced catalyst after the atom transfer reaction was more pronounced due to the high activity of the catalyst. This consumption of PEBr hindered the accurate determination of the deactivation rate constants. This difficulty was avoided by the in situ oxidation of the catalyst by exposing the system to air during the measurements. The reduced catalyst through atom transfer reactions was oxidized continuously and inactivated by oxygen in the air. Consequently, consumption of PEBr by the activation process was suppressed, and the mole ratio of PEBr and PETEMPO with time was almost constant.

Results

Activation Rate Constants. The measured rate constants are summarized for both the activation (Table 1) and the deactivation processes (Table 2). The activation rate constants were measured at 35 °C in acetonitrile. Acetonitrile is not a common solvent for ATRP but was used to obtain homogeneous catalyst solutions for all systems. The deactivation rate constants were also measured in acetonitrile, but at 75 °C because a higher temperature was required to ensure that the dissociation of PESG1 was fast enough to provide a reasonable amount of radicals.

Three alkyl halides were used as model compounds (Figure 7) for polymeric chain ends in ATRP: ethyl 2-bromoisobutyrate ([EBriB] as a model for poly(methyl methacrylate) [pMMA-Br]), methyl 2-bromopropionate ([MBrP] as a model for poly(methyl acrylate) [pMA-Br]), and 1-phenylethyl bromide ([PEBr] as a model for polystyrene [pSt-Br]).[7,30,31] Benzyl bromide [BzBr] was

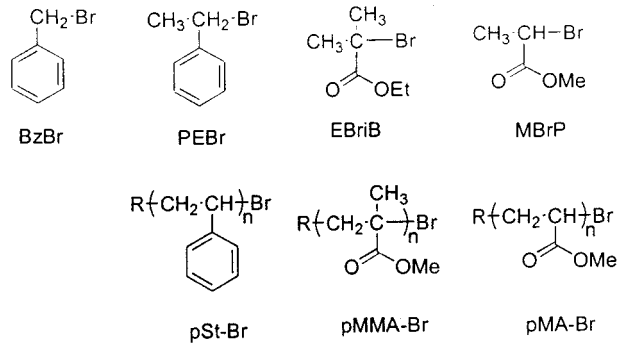

Figure 7. Model compounds of different polymeric chain ends in ATRP.

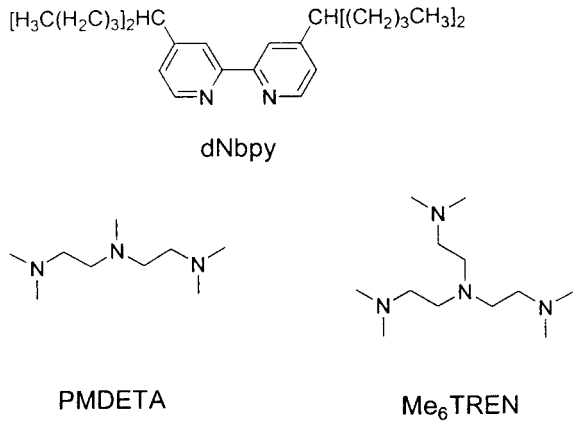

Figure 8. Multidentate nitrogen-based ligands.

also studied to enable a systematic comparison of the structural effect of alkyl groups on the activation rate constants. These alkyl halides are among the most widely used initiators in ATRP. Therefore, these model systems should provide information about the atom transfer process during both polymerization and initiation.

The order of the activation rate constants with CuBr/4,4′-di(5-nonyl)-2,2′-bipyridyl (dNbpy) was EBriB ≫ PEBr ≥ MBrP ≥ BzBr (entries 1−4 in Table 1). The order is similar using a different ligand, *N*,*N*,*N*′,*N*″,*N*″-pentamethyldiethylenetriamine (PMDETA) (entries 5−7 in Table 1). EBriB activates very fast with an activation rate constant approximately 10 times larger than that of the other model compounds.

To study the effect of ligands on the activation rate constants, we examined three representative ligands: dNbpy,[7,30,32] PMDETA,[33,34] and tris[2-(dimethylamino)-ethyl]amine (Me_6TREN)[35,36] (Figure 8). These ligands form active copper catalysts in the ATRP of many monomers. The activation rate constants increased in the order of dNbpy < PMDETA < Me_6TREN. The activation rate constant of Me_6TREN was measured using CuCl/PECl since the activation for the bromine-based system was too fast to measure with the given method. The CuCl/Me_6TREN promoted the almost fastest activation reaction even with the Cl-based system, despite being at least 10 times slower in the activation process than the corresponding Br-based system.[10]

The rates of activation were also influenced by solvents and transferred groups (X). More polar solvents accelerate the activation process. The activation rate constant of PEBr with CuBr/dNbpy in acetonitrile is more than 5 times larger than in ethyl acetate (entries 1 and 9 in Table 1). Entries 1 and 10 in Table 1 show the dependence of the activation rate constants on the transferred atoms. The activation rate constant of 1-PECl was about 1000 times smaller than that of 1-PEBr. At higher temperature, the difference in the activation rate constants between alkyl bromides and alkyl chlorides should be smaller due to larger activation energies of alkyl chlorides.[10,37]

Deactivation Rate Constants. Deactivation rate constants were measured only for the PE radical in acetonitrile at 75 °C (Table 2). Again, the three different ligands, dNbpy, PMDETA, and Me_6TREN, complexed with Cu(II)Br_2 were examined. The deactivation rate constants were not in the reverse order of the activation rate constants but decreased in the order of dNbpy > Me_6TREN > PMDETA.

The effect of solvents was more pronounced for the deactivation rate constants than for the activation rate constants. The deactivation rate constant in ethyl acetate is 10 times larger than that in acetonitrile. The deactivation rate constant of the Cl-based system is about 6 times smaller than that of the Br-based system (entries 1 and 5 in Table 2).

Discussion

Effect of Alkyl Groups. ATRP can polymerize various vinyl monomers; the most representative are styrenes, acrylates, and methacrylates. Detailed polymerization kinetic studies have been reported for these three monomers using the homogeneous catalyst, CuBr/dNbpy.[7,30,31] The rate of ATRP of MMA is faster than those of styrenes and other acrylates under the same reaction conditions and concentrations. The overall rate of ATRP is determined by the product of the propagation rate constant and the radical concentration, which is directly proportional to the equilibrium constant (K_{eq}) when excess deactivator is used. Since the propagation rate constant of MMA is smaller than that of acrylates and similar to that of styrenes,[38] the fast polymerization of MMA was attributed to the higher equilibrium constant. This explanation can be partially confirmed by the larger activation rate constant of EBriB.

Effect of Ligands. The ligand tunes the electronic, steric, and solubility properties of ATRP catalysts.[39] The data obtained here for three ligands clearly indicate that the rates of the activation and the deactivation can be adjusted using different ligands. Also, that the deactivation rate constants are not necessarily in the reverse order of the activation rate constants with different catalysts, in contrast to previous study with a series of tridentate ligands.[40] This suggests that the controlling factors in the activation and the deactivation processes are different, and it may be possible to develop a new catalyst with both a fast activation rate and a fast deactivation rate. Tripodal tetradentate ligands may be good candidates for such efficient ATRP catalysts. Estimated K_{eq} for different catalysts are in the order of Me_6TREN ≫ PMDETA > dNbpy, which is consistent with the order of the rates in the copper-catalyzed ATRP of methyl acrylate.[41]

Effect of Solvents. ATRP is conducted typically in bulk, but various solvents can also be used, such as organic solvents, water, supercritical CO_2, etc. In ATRP the solvent influences the polymerization rate as well as the level of control over the polymerization. When bipyridine-based catalysts are used, generally more polar media accelerate ATRP with less control over the polymerization. This significant solvent effect is rather

surprising since it is usually small in radical reactions including radical polymerization,[42] compared to ionic reactions.[43]

Polar solvent (i.e., acetonitrile) increased the rate of the activation process by a factor of 5 compared to that in less polar solvents (i.e., ethyl acetate). The deactivation rate constant was even more influenced by the solvent polarity. In ethyl acetate, the deactivation rate constant was 10 times larger than in acetonitrile. We currently attribute these observations to changes in the catalyst structure in different solvents. Detailed studies are in progress using kinetic studies as well as examination of the catalyst structures in different solvents. Nevertheless, we can conclude that the acceleration of ATRP in polar solvents with the CuBr/dNbpy catalyst is due to an increase in the activation rate constant as well as a decrease in the deactivation rate constant.

Effect of Transferred Group (X). Another important structural parameter in the ATRP process is the transferred atom (or group), represented by the halogen in this work. The use of different transferred atoms changes the rate of polymerization as well as the level of control over the polymerization.[39] ATRP of styrene with Cl-based system is slower with less control than those with Br-based system.[7] Entries 1 and 10 in Table 1 show that the activation rate constant of the Cl-based system is 1000 times smaller than the Br-based system. Entries 1 and 5 in Table 2 show that the deactivation rate constant of the Cl-based system is again about 6 times smaller than that of the Br-based system. The overall equilibrium is dominated by the differences in the activation rate constants, resulting in slower rates of polymerization for Cl-based system. At the same time, the slower deactivation rate in the Cl-based system leads to higher polydispersity.[7]

Comparison of Model Systems with Polymeric Systems. A question remains about how close the model systems are to polymeric systems. For the activation rate constant, the model system adequately represents the reactivity of the real polymeric system.[10,12] Goto and Fukuda compared the PEBr and polystyrene chain ends with CuBr/dNbpy[10] and showed that the activation rate constants of the model and real polymeric system are almost identical. The data for pSt chain ends are consistent with our extrapolated data for PEBr with CuBr/dNbpy.[12] However, in the case of EBriB, the reactivity may be lower than that of the pMMA chain end due to the B-strain effect, as previously discussed.[44,45]

Comparison of the deactivation rate constant of PE radicals with the estimated value for the deactivation rate constant of pSt chain ends provides some information about the difference between the model system from real polymeric system. The estimated deactivation rate constant for bromo-terminated pSt with CuBr/dNbpy was $1.1. \times 10^7\ M^{-1}\ s^{-1}$.[11] This value is smaller than the measured values for PE radical in both acetonitrile and ethyl acetate (entries 1 and 4 in Table 2). This may be due to different steric effects in the model compounds and the polymeric system or to different experimental conditions, including solvent and temperature. The nature of Cu(II) is influenced by temperature, solvent, and the presence of Cu(I) species.[46] This discrepancy between model and real systems needs to be examined further and will be the subject of our another study.

Conclusion. We have determined the activation and deactivation rate constants in model ATRP systems using HPLC or GC via kinetic isolation and competitive trapping, respectively. The rate constants of activation and deactivation for several model systems were examined under various conditions. The data obtained were consistent with those observed in the ATRP and provided further quantitative insight into ATRP processes. We already applied these methods to the systematic evaluation of the catalytic activities of complexes with different tridentate ligands[40] and ATRA mechanism study.[47]

Experimental Part

Materials. Cu(I)Br (99.999%, Aldrich), Cu(I)Cl (99.99%, Aldrich), and 2,2,6,6-tetramethylpiperidinyl-1-oxy (98% ACROS, TEMPO) were used without purification. 4,4′-Di(5-nonyl)-2,2′-bipyridine [dNbpy] was prepared as described previously.[7] All other chemicals were used as received. *N*,*N*-(2-Methylpropyl-1)-(1-diethylphosphono-2,2-dimethylpropyl-1-)-*N*-oxyl (SG1) was provided by Elf Atochem. 1-(2,2,6,6-Tetramethylpiperidinyloxy)-1-phenylethane (PETEMPO) and 1-(*N*,*N*-(2-methylpropyl-1)-(1-diethylphosphono-2,2-dimethylpropyl-1-)-*N*-oxyl)-1-phenylethane (PESG1) were prepared following reported procedure.[26,48] All prepared alkoxyamines were stored at −20 °C.

Activation Rate Constant Measurements. The Cu(I) complexes were prepared in situ under an N_2 atmosphere by adding 2 mL of deoxygenated acetonitrile to 40.8 mg of dNbpy (0.1 mmol), 15.6 mg of TEMPO (0.1 mmol), and 7.2 mg of CuBr (5.0×10^{-2} mmol) in a Schlenk flask. After three freeze−pump−thaw cycles and stirring for 30 min at 35 °C, 0.5 mL of deoxygenated PEBr and biphenyl stock solution (5.0×10^{-3} M each in acetonitrile) was added to the Schlenk flask via a degassed syringe. A sample was taken immediately for the reference, and other samples were taken at timed intervals. The samples taken were passed through alumina in order to remove the catalyst. The consumption of alkyl halide was determined with either reverse-phase HPLC or gas chromatography. HPLC was performed using a Shimadzu LC 10AD pump, 712 WISP autosampler, Waters Nova-Pak C18 column (3.9 × 150 mm), and Waters 486 tunable absorbance detector (λ = 220 nm) at 35 °C by the elution of an acetonitrile and water mixture (55:45 vol %). The retention times of TEMPO, PEBr, biphenyl, and PETEMPO were 3.6, 6.0, 8.8, and 67.0 min, respectively. GC was performed using a Shimadzu GC-17A, AOC-20i autosampler, and J &W Scientific DB 608 column (30 m × 0.53 mm) with a FID detector. The injector and detector temperature was kept constant at 250 °C. The temperature program for GC column was as follows: initial temperature, 45 °C, 0 min; ramp, 5 °C/min; final temperature, 180 °C, 0 min. The retention times of MBP, EBiB, PEBr, BzBr, biphenyl, and TEMPO were 4.2, 5.5, 12.1, 10.8, 18.8, and 10.3 min, respectively. All data were collected and processed with Shimadzu Class VP chromatographic data system (version 4.2).

Deactivation Rate Constant Measurements. To 6.7 mg of $CuBr_2$ (3.0×10^{-2} mmol) and 24.5 mg of dNbpy (6.0×10^{-2} mmol) in 2.40 mL of acetonitrile were added 0.30 mL of TEMPO stock solution (0.030 M in acetonitrile) and 0.30 mL of PESG1 and biphenyl stock solution (0.010 M each in acetonitrile). The solution was deoxygenated with three freeze−pump−thaw cycles. After taking a sample, the solution was heated to 75 °C in an oil bath, and samples were taken at timed intervals. The samples were passed through alumina in order to remove the catalyst. The concentration of PEBr, PESG1, and PETEMPO was determined using reverse-phase HPLC as described above. The retention times of TEMPO, PEBr, biphenyl, PESG1A, PESG1B, and PETEMPO were 3.6, 6.0, 8.8, 44.2, 58.6, and 67.0 min, respectively.

Acknowledgment. The financial support from the National Science Foundation (CHE-0096601) and from ATRP Consortium is gratefully acknowledged. We also thank Atofina for the generous donation of SG1.

References and Notes

(1) This work was partially presented at 219th ACS Meeting, San Francisco, CA, March 2000, and 221th ACS Meeting, San Diego, CA, April 2001.
(2) Iqbal, J.; Bhatia, B.; Nayyar, N. K. *Chem. Rev.* **1994**, *94*, 519−564.
(3) Curran, D. P. *Synthesis* **1988**, 489−513.
(4) Wang, J. S.; Matyjaszewski, K. *J. Am. Chem. Soc.* **1995**, *117*, 5614−5615.
(5) Kato, M.; Kamigaito, M.; Sawamoto, M.; Higashimura, T. *Macromolecules* **1995**, *28*, 1721−1723.
(6) Percec, V.; Barboiu, B. *Macromolecules* **1995**, *28*, 7970−7972.
(7) Matyjaszewski, K.; Patten, T. E.; Xia, J. *J. Am. Chem. Soc.* **1997**, *119*, 674−680.
(8) Matyjaszewski, K. *Chem. Eur. J.* **1999**, *5*, 3095−3102.
(9) Patten, T. E.; Matyjaszewski, K. *Acc. Chem. Res.* **1999**, *32*, 895−903.
(10) Goto, A.; Fukuda, T. *Macromol. Rapid Commun.* **1999**, *20*, 633−636.
(11) Ohno, K.; Goto, A.; Fukuda, T.; Xia, J.; Matyjaszewski, K. *Macromolecules* **1998**, *31*, 2699−2701.
(12) Paik, H.-j.; Matyjaszewski, K. *Polym. Prepr. (Am. Chem. Soc., Div. Polym. Chem.)* **2000**, *41* (1), 470−471.
(13) Chambard, G.; Klumperman, B.; German, A. L. *Macromolecules* **2000**, *33*, 4417−4421.
(14) Matyjaszewski, K. *Macromol. Symp.* **1996**, *111*, 47−61.
(15) Matyjaszewski, K. *J. Macromol. Sci., Pure Appl. Chem.* **1997**, *A34*, 1785−1801.
(16) Jenkins, C. L.; Kochi, J. K. *J. Am. Chem. Soc.* **1972**, *94*, 856−865.
(17) Skene, W. G.; Belt, S. T.; Connolly, T. J.; Hahn, P.; Scaiano, J. C. *Macromolecules* **1998**, *31*, 9103−9105.
(18) Marque, S.; Mercier, C. L.; Tordo, P.; Fischer, H. *Macromolecules* **2000**, *33*, 4403−4410.
(19) Kothe, T.; Marque, S.; Martschke, R.; Popov, M.; Fischer, H. *J. Chem. Soc., Perkin Trans. 2* **1998**, *7*, 1553−1559.
(20) Bon, S. A. F.; Chambard, G.; German, A. L. *Macromolecules* **1999**, *32*, 8269−8276.
(21) Matyjaszewski, K.; Davis, K.; Patten, T. E.; Wei, M. *Tetrahedron* **1997**, *53*, 15321−15329.
(22) Li, I.; Howell, B. A.; Matyjaszewski, K.; Shigemoto, T.; Smith, P. B.; Priddy, D. B. *Macromolecules* **1995**, *28*, 6692−6693.
(23) Ohno, K.; Tsujii, Y.; Fukuda, T. *Macromolecules* **1997**, *30*, 2503−2506.
(24) Skene, W. G.; Scaiano, J. C.; Listigovers, N. A.; Kazmaier, P. M.; Georges, M. K. *Macromolecules* **2000**, *33*, 5065−5072.
(25) Beckwith, A. L. J.; Bowry, V. W.; Ingold, K. U. *J. Am. Chem. Soc.* **1992**, *114*, 4983−4992.
(26) Mercier, C. L.; Lutz, J.-F.; Marque, S.; Moigne, F. L.; Tordo, P.; Lacroix-Desmaze, P.; Boutevin, B.; Couturier, J.-L.; Guerret, O.; Martschke, R.; Sobek, J.; Fischer, H. In *Controlled/Living Radical Polymerization: Progress in ATRP, NMP and RAFT*; Matyjaszewski, K., Ed.; ACS Symp. Ser. 768; American Chemical Society: Washington, DC, 2000; p 108.
(27) Benoit, D.; Grimaldi, S.; Finet, J. P.; Tordo, P.; Fontanille, M.; Gnanou, Y. *ACS Symp. Ser.* **1998**, *685*, 225−235.
(28) Benoit, D.; Grimaldi, S.; Robin, S.; Finet, J.-P.; Tordo, P.; Gnanou, Y. *J. Am. Chem. Soc.* **2000**, *122*, 5929−5939.
(29) Benoit, D.; Chaplinski, V.; Braslau, R.; Hawker, C. J. *J. Am. Chem. Soc.* **1999**, *121*, 3904−3920.
(30) Davis, K. A.; Paik, H.-j.; Matyjaszewski, K. *Macromolecules* **1999**, *32*, 1767−1776.
(31) Wang, J.-L.; Grimaud, T.; Matyjaszewski, K. *Macromolecules* **1997**, *30*, 6507−6512.
(32) Grimaud, T.; Matyjaszewski, K. *Macromolecules* **1997**, *30*, 2216−2218.
(33) Xia, J.; Matyjaszewski, K. *Macromolecules* **1997**, *30*, 7697−7700.
(34) Davis, K. A.; Matyjaszewski, K. *Macromolecules* **2000**, *33*, 4039−4047.
(35) Xia, J.; Gaynor, S. G.; Matyjaszewski, K. *Macromolecules* **1998**, *31*, 5958−5959.
(36) Queffelec, J.; Gaynor, S. G.; Matyjaszewski, K. *Macromolecules* **2000**, *33*, 8629−8639.
(37) Peng, Z.; Paik, H.-j.; Matyjaszewski, K. Manuscript in preparation.
(38) Van Herk, A. M. *J. Macromol. Sci., Rev. Macromol. Chem. Phys.* **1997**, *C37*, 633−648.
(39) Matyjaszewski, K. In *Controlled Radical Polymerization*; Matyjaszewski, K., Ed.; ACS Symp. Ser. 685; American Chemical Society: Washington, DC, 1998; p 258.
(40) Matyjaszewski, K.; Göbelt, B.; Paik, H.-j.; Horwitz, C. P. *Macromolecules* **2001**, *34*, 430−440.
(41) Qiu, J.; Matyjaszewski, K.; Thouin, L.; Amatore, C. *Macromol. Chem. Phys.* **2000**, *201*, 1625−1631.
(42) Moad, G.; Solomon, D. H. *The Chemistry of Free Radical Polymerization*; Pergamon: Oxford, 1995.
(43) Reichardt, C. *Solvents and Solvent Effects in Organic Chemistry*, 2nd ed.; VCH: Weinheim, Federal Republic of Germany, 1988.
(44) Wang, J.-L.; Grimaud, T.; Shipp, D. A.; Matyjaszewski, K. *Macromolecules* **1998**, *31*, 1527.
(45) Ando, T.; Kamigaito, M.; Sawamoto, M. *Tetrahedron* **1997**, *53*, 15445.
(46) Qiu, J.; Pintauer, T.; Gaynor, S.; Matyjaszewski, K. *Polym. Prepr.* **1999**, *40* (2), 420−421. Pintauer, T.; Qiu, J.; Kickelbick, G.; Matyjaszewski, K. *Inorg. Chem.* **2001**, *40*, 2818−2824.
(47) Matyjaszewski, K.; Paik, H.-j.; Shipp, D. A.; Isobe, Y.; Okamoto, Y. *Macromolecules* **2001**, *34*, 3127−2129.
(48) Matyjaszewski, K.; Woodworth, B. E.; Zhang, X.; Gaynor, S. G.; Metzner, Z. *Macromolecules* **1998**, *31*, 5955−5957.

MA010185+